some other, less important internal contacts.

We turn, finally, to what is the most remarkable feature of the $Re_2Cl_4(dmpe)_2$ molecule, namely, that it has an eclipsed rotational conformation, despite the fact that there is no barrier to rotation about the triple Re-Re bond. In the case of the isostructural $W_2Cl_4(dmpe)_2$, this might have been attributed solely to the rotational barrier inherent in the W-W quadruple bond, but the preference of $Re_2Cl_4(dmpe)_2$ for the same structure shows that there are other important forces at work to favor this structure. We hope to provide, in a future report, a detailed and perhaps quantitative analysis of the conformational behavior of these molecules, but we can give here a brief qualitative description of the key features, which are the following:

(i) If the chelate ring conformations are kept constant and rotation about the M-M bond is carried out, the result is an enormous increase in the repulsive contacts between atoms on the two different ends of the molecule, especially one methyl-methyl and two methyl-chlorine contacts. The methyl to methyl distance at a rotation angle of 45° would be ca. 0.9 Å (C to C), an obviously impossible situation; in the eclipsed conformation actually adopted, the closest methyl-methyl contacts are ca. 3.8 Å and all other nonbonded distances are also acceptable.

(ii) If we were to flip both five-membered rings so that the envelopes bend the opposite way, i.e., with the planar PCCP units directed distally, we generate a large number of close contacts even in the eclipsed conformation (mainly, *four* methyl-chlorine contacts of less than 2.0 Å) and in the staggered conformation there are four very short methyl-methyl contacts as well as several short methyl-chlorine contacts.

In summary, the conformational characteristics of both of the α-$M_2Cl_4(dmpe)_2$ molecules appear to be dictated primarily by the nonbonded interactions between the ligand atoms (especially the methyl groups) and, in particular, the eclipsed rotational conformation about the M-M bonds occurs whether there is (in the W_2 compound) or is not (in the Re_2 compound) a δ bond. This case is therefore similar in principle to that of the $M_2X_4(PR_3)_4$ molecules, where an eclipsed conformation about the metal-metal bond is required by the ligand-ligand repulsions, regardless of whether there is (in the Mo_2 and W_2 compounds) or is not (in the Re_2 compounds) a δ bond.

Acknowledgment. Support from the National Science Foundation (Grant No. CHE 82-8211407 to F.A.C. and Grant No. 82-06117 to R.A.W.) is gratefully acknowledged.

Registry No. **1**, 58298-10-5; **2**, 96808-01-4; $Re_2Cl_6(P\text{-}n\text{-}Bu_3)_2$, 38832-70-1; $(n\text{-}Bu_4N)_2Re_2Cl_8$, 14023-10-0; Re, 7440-15-5.

Supplementary Material Available: Tables of structure factors and anisotropic thermal parameters for $Re_2Cl_4(dppm)_2$ and $Re_2Cl_4(dmpe)_2$ and full lists of bond distances and angles for $Re_2Cl_4(dppm)_2$ (21 pages). Ordering information is given on any current masthead page.

Contribution from the Department of Chemistry,
University of Minnesota, Minneapolis, Minnesota 55455

Synthesis and Characterization of the Novel Gold-Iridium Cluster $[IrAu_4(H)_2(PPh_3)_6]BF_4$

ALBERT L. CASALNUOVO, JOSEPH A. CASALNUOVO, PER V. NILSSON, and LOUIS H. PIGNOLET*

Received November 8, 1984

The novel new dihydride iridium-gold cluster complex $[IrAu_4(H)_2(PPh_3)_6]BF_4$ (**1**) was synthesized from the reaction of an acetone solution of $[IrAu_3(PPh_3)_5NO_3]BF_4$ with 1 atm of H_2. Complex **1** was isolated in good yield and was characterized in solution by ^1H and ^{31}P NMR spectroscopy and in the solid state by single-crystal X-ray diffraction. The cluster crystallizes as a 1.5 CH_2Cl_2 solvate in the monoclinic space group $C2/c$ (a = 53.46 (2) Å, b = 14.270 (8) Å, c = 29.228 (9) Å, β = 113.12 (3)°, Z = 8; V = 20 506 Å^3 and R = 0.052 for 4367 observed reflections with $F_o^2 \geq 3\sigma(F_o^2)$]. The molecular structure of the $[IrAu_4(H)_2(PPh_3)_6]^+$ cation consists of an approximately trigonal-bipyramidal (TBP) $IrAu_4$ core with an $Ir(PPh_3)_2$ unit occupying an equatorial position. The four $AuPPh_3$ units occupy the axial positions and the two remaining equatorial sites. The major deviation from ideal TBP geometry is caused by the shorter Ir-Au distances (average 2.690 (2) Å) compared with the bonded (eq-eq and eq-ax) Au-Au separations (average 2.920 (2) Å). The two hydrides were not located by the X-ray analysis but are thought to be bridging Ir-axial Au bonds. The solution ^1H NMR data tend to support this assignment, however, with some uncertainty, and a terminal Ir-H bonding description is also possible. The complex is fluxional in solution. Variable-temperature ^{31}P NMR data show that a process that interchanges the axial and equatorial Au sites is occurring.

Introduction

During the past several years there has been considerable interest in the synthesis of mixed-metal gold cluster compounds.[1-15] Our research group has been primarily interested in iridium- and rhodium-gold clusters that contain phosphine and hydrido ligands and their potential usefulness in catalysis.[1,13-15] For example, $[IrAu_2(H)(PPh_3)_4NO_3]BF_4$ (**1**)[1] and $[IrAu_3(PPh_3)_5NO_3]BF_4$ (**2**)[13] have been synthesized and characterized by single-crystal X-ray

(1) Casalnuovo, A. L.; Pignolet, L. H.; van der Velden, J. W. A.; Bour, J. J.; Steggerda, J. J. *J. Am. Chem. Soc.* **1983**, *105*, 5957.
(2) Steggerda, J. J.; Bour, J. J.; van der Velden, J. W. A. *Recl. Trav. Chim. Pays-Bas* **1982**, *101*, 164.
(3) Mingos, D. M. P. *Proc. R. Soc. London, Ser. A* **1982**, *308*, 75. Hall, K. P.; Mingos, D. M. P. *Prog. Inorg. Chem.* **1984**, *32*, 237.
(4) Johnson, B. F. G.; Lewis, J.; Nicholls, J. N.; Puga, J.; Whitmire, K. H. *J. Chem. Soc., Dalton Trans.* **1983**, 787.
(5) Teo, B. K.; Keating, K. *J. Am. Chem. Soc.* **1984**, *106*, 2224.
(6) Lehner, H.; Matt, D.; Pregosin, P. S.; Venanzi, L. M. *J. Am. Chem. Soc.* **1982**, *104*, 6825.
(7) Green, M.; Orpen, A. G.; Salter, I. D.; Stone, F. G. A. *J. Chem. Soc., Chem. Commun.* **1982**, 813.
(8) Lauher, J. W.; Wald, K. *J. Am. Chem. Soc.* **1981**, *103*, 7648.
(9) Lavigne, G.; Papageorgiou, F.; Bonnet, J.-J. *Inorg. Chem.* **1984**, *23*, 609 and references therein.
(10) Evans, D. G.; Mingos, D. M. P. *J. Organomet. Chem.* **1982**, *232*, 171 and references therein.
(11) Braunstein, P.; Lehner, H.; Matt, D.; Tiripicchio, A.; Tiripicchio-Camellini, M. *Angew. Chem., Int. Ed. Engl.* **1984**, *23*, 304 and references cited therein.
(12) Hutton, A. T.; Pringle, P. G.; Shaw, B. L. *Organometallics* **1983**, *2*, 1889.
(13) Casalnuovo, A. L.; Laska, T.; Nilsson, P. V.; Olofson, J.; Pignolet, L. H.; Bos, W.; Bour, J. J.; Steggerda, J. J. *Inorg. Chem.* **1985**, *24*, 182.
(14) Casalnuovo, A. L.; Laska, T.; Nilsson, P. V.; Olofson, J.; Pignolet, L. H. *Inorg. Chem.* **1985**, *24*, 233.
(15) McNair, R. J.; Nilsson, P. V.; Pignolet, L. H. *Inorg. Chem.* **1985**, *24*, 1935.
(16) NMCSIM is described in the Nicolet Magnetics Corp. 1280 program manual.

0020-1669/85/1324-2554$01.50/0

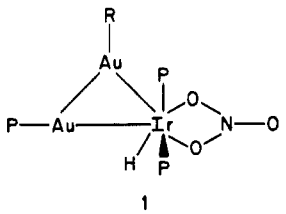

1

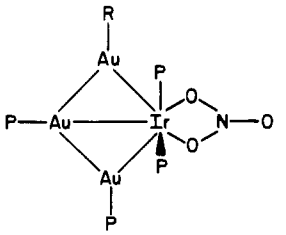

2

diffraction. These complexes were synthesized by the reaction of $AuPPh_3NO_3$ with $[Ir(H)_2(PPh_3)_2((CH_3)_2CO)_2]BF_4$ in acetone solution. Compound **1** is thermally unstable in acetone solution and slowly reacts at 25 °C to give **2**. Complex **2** has an unusual planar $IrAu_3$ grouping and is reactive toward small molecules such as CO and H_2. In this paper we report the reaction of **2** with H_2 in acetone solution and the isolation and characterization of the novel product $[IrAu_4(H)_2(PPh_3)_6]BF_4$ (**3**).

Experimental Section

Physical Measurements. ^1H and $^{31}P\{^1H\}$ NMR spectra were recorded at 300 and 121.5 MHz, respectively, with the use of a Nicolet NT-300 spectrometer. ^{31}P chemical shifts are reported in ppm relative to the internal standard trimethyl phosphate (TMP). ^{31}P NMR simulations were carried out with the use of the Nicolet program NMCSIM. Infrared spectra were recorded on a Beckman Model 4250 grating spectrometer with the use of KBr disks. Solvents were dried and distilled prior to use. $Au(PPh_3)NO_3$[17] and $[IrAu_3(PPh_3)_5NO_3](BF_4)$[13] were prepared as described in the literature. The preparation of $[IrAu_4(H)_2(PPh_3)_6](BF_4)$ was carried out under a purified N_2 atmosphere with use of standard Schlenk techniques; however, CH_2Cl_2, THF, and acetone solutions were not air sensitive.

Preparation of $[IrAu_4(H)_2(PPh_3)_6](BF_4)$ (3). A red-brown solution of 75 mg of **2** in 3 mL of CH_2Cl_2 was stirred vigorously under 1 atm of H_2 at 23 °C for 45 min. Within 4 min the initial red-brown color of the solution faded to a golden yellow and then gradually changed to red-orange over the next 15 min. A yellow-orange powder precipitated from this stirring solution upon the addition of 25 mL of diethyl ether. This powder was redissolved in a minimum amount of THF and filtered through diatomaceous earth. The THF was removed in vacuo and the remaining yellow-orange residue was crystallized from CH_2Cl_2/Et_2O. The crystallization was best carried out with a very minimum amount of CH_2Cl_2, since **3** was very soluble in this solvent. **3** precipitated as a combination of very thin golden fibers and large red-orange plates. The latter crystals were used for the X-ray analysis; however, both materials gave identical ^1H and $^{31}P\{^1H\}$ NMR spectra. The red-orange plates were found to slowly lose CH_2Cl_2 of crystallization. Samples of **3** were therefore dried in vacuo prior to determining the elemental analysis. Yields typically ranged from 55 to 60% based on Ir. $^{31}P\{^1H\}$ NMR (acetone, 23 °C): δ 46.5, triplet, J(P–P) = 33 Hz, int = 2; ~33.5, broad singlet, int = 1. ^1H NMR (acetone-d_6, 23 °C): δ = −5.71, multiplet. Anal. Calcd for $IrAu_4C_{108}H_{92}P_6BF_4$: C, 49.08; H, 3.51; F, 2.88. Found: C, 48.58; H, 3.44; F, 3.08. The infrared spectrum of **3** in KBr indicated the presence of BF_4^- (ν(B–F) = 1050 cm^{-1} (s) but gave no evidence of free NO_3^-.

X-ray Structure Determination. Collection and Reduction of X-ray Data. A summary of crystal and intensity collection data is presented in Table I. Crystals of $[Au_4Ir(PPh_3)_6(H)_2]BF_4$ were found to lose solvent upon removal from CH_2Cl_2–$(C_2H_5)_2O$ solution. This solvent loss was rapid and caused single crystals to fracture. Therefore, the crystal used for data collection was mounted inside a 0.2-mm capillary that was half-filled with solvent. The crystal was subsequently found to contain 1.5 CH_2Cl_2 solvate molecules per Au_4Ir cluster. The crystal was found to belong to the *C*-centered monoclinic crystal class by the Enraf-Nonius CAD 4-SDP peak search, centering, and indexing programs and by a Delaunay reduction calculation.[18] The space group $C2/c$ (No. 15) was chosen on the basis of systematic absences observed during data collection and was verified by successful solution and refinement (vide infra). The unit cell dimensions were determined by least-squares refinement of the angular settings of 25 peaks centered on the diffractometer. Background counts were measured at both ends of the scan range with the use of an ω scan, equal, at each side, to one-fourth of the scan range of the peak. The intensities of three standard reflections were measured every 1.5 h of X-ray exposure, and no decay with time was noted. The data were corrected for Lorentz, polarization, and background effects. The effects of absorption were included with use of the empirical absorption program EAC (ψ scan data).[18]

Table I. Summary of Crystal Data and Intensity Collection for $[Au_4Ir(PPh_3)_6(H)_2]BF_4 \cdot 1.5CH_2Cl_2$

Crystal Parameters	
cryst syst	monoclinic
space group	$C2/c$ (No. 15)
cryst dimens, mm^3	0.2 × 0.1 × 0.25
cell parameters (25 °C)	
a, Å	53.46 (2)
b, Å	14.270 (8)
c, Å	29.228 (9)
α, deg	90
β, deg	113.12 (3)
γ, deg	90
V, $Å^3$	20 506 (1)
Z	8
calcd density, g cm^{-3}	1.822
abs coeff, cm^{-3}	72.3
max, min, av transmission factors	1.0, 0.54, 0.87
formula	$C_{108}H_{92}BF_4P_6Au_4Ir \cdot 1.5CH_2Cl_2$
fw	2812.52
Measurement of Intensity Data (25 °C)	
diffractometer	CAD-4
radiation	Mo K$\bar{\alpha}$ (λ = 0.710 69 Å), graphite monochromatized
scan type; range, 2θ, deg	ω; 0–21
obsd reflcns[a]	4367 ($F_o^2 \geq 3\sigma(F_o^2)$)
refinement by full-matrix least squares	
no. of parameters	543
R[b]	0.052
R_w[b]	0.056
GOF[b]	1.38
p[a]	0.04

[a] The intensity data were processed as described in: "CAD4 and SDP-PLUS User's Manual"; B. A. Frenz & Associates, Inc.: College Station, TX, 1982. The net intensity $I = [K/NPI](C - 2B)$, where K = 20.1166 × attenuator factor, NPI = ratio of fastest possible scan rate to scan rate for the measurement, C = total count, and B = total background count. The standard deviation in the net intensity is given by $[\sigma(I)]^2 = (K/NPI)^2[C + 4B + (pI)^2]$, where p is a factor used to downweight intense reflections. The observed structure factor amplitude F_o is given by $F_o = (I/Lp)^{1/2}$, where Lp = Lorentz and polarization factors. The $\sigma(I)$'s were converted to the estimated errors in the relative structure factors $\sigma(F_o)$ by $\sigma(F_o) = {}^1/_2[\sigma(I)/I]F_o$. [b] The function minimized was $\sum w(|F_o| - |F_c|)^2$, where $w = 1/[\sigma(F_o)]^2$. The unweighted and weighted residuals are defined as $R = (||F_o| - |F_c||)/\sum|F_o|$ and $R_w = [(\sum w(|F_o| - |F_c|)^2/(\sum w|F_o|)^2]^{1/2}$. The error in an observation of unit weight (GOF) is $[\sum w(|F_o| - |F_c|)^2/(NO - NV)]^{1/2}$, where NO and NV are the number of observations and variables, respectively.

Solution and Refinement of the Structure. The structure was solved by conventional heavy-atom techniques. The metal atoms were located by Patterson synthesis. Full-matrix least-squares refinement and difference-Fourier calculations were used to locate all remaining non-hydrogen atoms. Hydrogen atoms were not located and were not included in any calculations. The atomic scattering factors were taken from the usual tabulation,[19] and the effects of anomalous dispersion were included in F_c by using the Cromer and Ibers[20] values of $\Delta f'$ and $\Delta f''$. Corrections for extinction were not applied. The final difference-Fourier map did not reveal significant residual electron density. One CH_2Cl_2 molecule was

(17) Malatesta, L.; Naldini, L.; Simonetta, G.; Cariati, F. *Coord. Chem. Rev.* **1966**, *1*, 255.

(18) All calculations were carried out on PDP 8A and 11/34 computers with use of the Enraf-Nonius CAD 4-SDP-PLUS programs. This crystallographic computing package is described by: Frenz, B. A. In "Computing in Crystallography"; Schenk, H.; Olthof-Hazekamp, R., van Konigsveld, H.; Bassi, G. C., Eds.; Delft University Press: Delft, Holland, 1978; pp 64–71. "Structure Determination Package and SDP-PLUS User's Guide"; B. A. Frenz & Associates, Inc.: College Station, TX, 1982.

(19) Cromer, D. T.; Waber, J. T. "International Tables for X-ray Crystallography"; Kynoch Press: Birmingham, England, 1974; Vol. IV, Table 2.2.4. Cromer, D. T. Ibid., Table 2.3.1.

(20) Cromer, D. T.; Ibers, J. A. In ref 19.

Table II. Positional Parameters and Their Estimated Standard Deviations

atom	*x*	*y*	*z*	*B*, Å^{2a}	atom	*x*	*y*	*z*	*B*, Å^{2a}
Ir	0.15471 (2)	0.31898 (9)	0.11764 (5)	2.75 (3)	C1J	0.0427 (5)	0.214 (2)	0.111 (1)	3.0 (7)*
Au1	0.10894 (2)	0.35299 (9)	0.03731 (5)	3.22 (3)	C6M	0.2076 (6)	0.071 (2)	0.227 (1)	4.8 (9)*
Au2	0.13339 (3)	0.15595 (9)	0.07959 (6)	3.49 (3)	C1N	0.2217 (5)	0.221 (2)	0.169 (1)	2.8 (6)*
Au3	0.15435 (2)	0.2753 (1)	0.02564 (5)	3.50 (3)	C2N	0.2463 (6)	0.243 (2)	0.206 (1)	4.6 (8)*
Au4	0.10695 (2)	0.2900 (1)	0.12632 (5)	3.91 (4)	C3N	0.2702 (7)	0.218 (3)	0.196 (1)	7 (1)*
P1	0.0707 (2)	0.3926 (6)	−0.0315 (3)	3.4 (2)*	C4N	0.2681 (7)	0.185 (3)	0.151 (1)	8 (1)*
P2	0.1223 (2)	0.0025 (6)	0.0552 (3)	3.7 (2)*	C5N	0.2442 (6)	0.162 (3)	0.116 (1)	6 (1)*
P3	0.1643 (2)	0.2593 (7)	−0.0428 (3)	4.1 (2)*	C6N	0.2179 (6)	0.181 (3)	0.121 (1)	6 (1)*
P4	0.0717 (2)	0.2828 (7)	0.1502 (3)	4.2 (2)*	C1P	0.2039 (6)	0.303 (2)	0.244 (1)	4.9 (8)*
P5	0.1901 (1)	0.2444 (6)	0.1805 (3)	2.9 (2)*	C2P	0.1994 (6)	0.269 (2)	0.283 (1)	4.5 (8)*
P6	0.1631 (2)	0.4798 (7)	0.1289 (3)	3.8 (2)*	C3P	0.2105 (5)	0.318 (2)	0.327 (1)	4.0 (8)*
C1A	0.0503 (5)	0.486 (2)	−0.019 (1)	3.7 (7)*	C4P	0.2251 (6)	0.406 (2)	0.329 (1)	5.4 (9)*
C2A	0.0485 (5)	0.482 (2)	0.028 (1)	3.0 (7)*	C5P	0.2288 (5)	0.440 (2)	0.290 (1)	4.0 (8)*
C3A	0.0341 (6)	0.553 (2)	0.042 (1)	5.4 (9)*	C6P	0.2183 (6)	0.393 (2)	0.246 (1)	4.2 (8)*
C4A	0.0223 (6)	0.622 (2)	0.006 (1)	5.5 (9)*	C1Q	0.1442 (6)	0.558 (2)	0.076 (1)	4.4 (8)*
C5A	0.0238 (6)	0.629 (2)	−0.037 (1)	5.6 (9)*	C2Q	0.1558 (5)	0.588 (2)	0.046 (1)	3.9 (8)*
C6A	0.0386 (6)	0.560 (2)	−0.054 (1)	4.9 (9)*	C3Q	0.1387 (6)	0.352 (3)	0.505 (1)	6 (1)*
C1B	0.0787 (5)	0.432 (2)	−0.081 (1)	3.9 (8)*	C4Q	0.1120 (6)	0.667 (2)	−0.000 (1)	5.2 (9)*
C2B	0.1040 (5)	0.477 (2)	−0.073 (1)	3.8 (8)*	C5Q	0.1005 (6)	0.638 (3)	0.029 (1)	5.8 (9)*
C3B	0.1101 (6)	0.501 (2)	−0.112 (1)	4.4 (8)*	C6Q	0.3838 (5)	0.080 (2)	0.432 (1)	3.9 (8)*
C4B	0.0919 (7)	0.502 (3)	−0.161 (1)	6 (1)*	C1R	0.1983 (6)	0.523 (3)	0.139 (1)	5.8 (9)*
C5B	0.0661 (6)	0.459 (2)	−0.172 (1)	5.2 (9)*	C2R	0.2937 (7)	0.112 (3)	0.339 (1)	7 (1)*
C4F	0.0743 (7)	0.062 (3)	0.390 (1)	6 (1)*	C3R	0.2327 (7)	0.640 (3)	0.163 (1)	8 (1)*
C5F	0.0934 (7)	0.015 (3)	−0.095 (1)	6 (1)*	C4R	0.2497 (7)	0.590 (3)	0.144 (1)	7 (1)*
C6F	0.1068 (6)	0.036 (2)	−0.046 (1)	4.9 (8)*	C5R	0.2399 (6)	0.500 (2)	0.126 (1)	4.3 (8)*
C1G	0.1388 (5)	0.222 (2)	−0.101 (1)	3.9 (7)*	C6R	0.2141 (6)	0.463 (2)	0.123 (1)	4.7 (8)*
C2G	0.1476 (7)	0.172 (3)	−0.134 (1)	7 (1)*	C1S	0.1572 (5)	0.541 (2)	0.180 (1)	3.8 (7)*
C3G	0.1281 (7)	0.149 (3)	−0.184 (1)	6 (1)*	C2S	0.1555 (7)	0.486 (3)	0.218 (1)	6 (1)*
C4G	0.1008 (7)	0.182 (3)	−0.196 (1)	8 (1)*	C3S	0.1488 (6)	0.529 (3)	0.257 (1)	6 (1)*
C5G	0.0919 (7)	0.230 (3)	−0.163 (1)	7 (1)*	C4S	0.3554 (7)	0.129 (3)	0.247 (1)	6 (1)*
C6G	0.1134 (6)	0.248 (3)	−0.114 (1)	6 (1)*	C5S	0.3527 (6)	0.180 (3)	0.280 (1)	5.8 (9)*
C1H	0.1921 (6)	0.177 (2)	−0.031 (1)	5.7 (9)*	C6S	0.1515 (6)	0.644 (2)	0.179 (1)	5.6 (9)*
C2H	0.2160 (6)	0.197 (3)	−0.042 (1)	5.8 (9)*	B	0.250 (4)	−0.30 (1)	−0.014 (7)	16 (7)*
C3H	0.2364 (6)	0.132 (2)	−0.034 (1)	5.2 (9)*	F1	0.219 (2)	−0.279 (8)	−0.009 (4)	26 (4)*
C4H	0.2349 (7)	0.052 (3)	−0.013 (1)	7 (1)*	F2	0.223 (2)	−0.269 (8)	−0.025 (4)	27 (5)*
C5H	0.2120 (7)	0.024 (3)	−0.003 (1)	7 (1)*	F3	0.223 (2)	−0.229 (8)	−0.037 (4)	28 (5)*
C6H	0.1903 (6)	0.091 (3)	−0.010 (1)	5.9 (9)*	F4	0.239 (2)	−0.188 (8)	−0.052 (4)	27 (5)*
C1I	0.1764 (6)	0.373 (2)	−0.056 (1)	4.6 (8)*	C12	0.181 (2)	−0.101 (8)	−0.080 (4)	29 (5)*
C2I	0.1869 (6)	0.437 (3)	−0.015 (1)	5.8 (9)*	C44	0.000	1.018 (6)	0.250	12 (3)*
C3I	0.1953 (7)	0.523 (3)	−0.026 (1)	8 (1)*	Cl1	0.1785 (4)	−0.076 (2)	−0.1462 (8)	16.5 (7)*
C4I	0.1950 (6)	0.541 (3)	−0.072 (1)	6 (1)*	Cl2	0.1605 (6)	0.214 (2)	0.403 (1)	27 (1)*
C5I	0.1845 (6)	0.479 (3)	−0.114 (1)	6 (1)*	Cl4	0.0235 (8)	0.992 (3)	0.241 (2)	16 (1)*
C6I	0.1747 (7)	0.394 (3)	−0.104 (1)	7 (1)*					

[a] Atoms marked with an asterisk were refined isotropically. Anisotropically refined atoms are given in the form of the isotropic equivalent thermal parameter defined as $^4/_3[a^2\beta_{1,1} + b^2\beta_{2,2} + c^2\beta_{3,3} + ab(\cos\gamma)\beta_{1,2} + ac(\cos\beta)\beta_{1,3} + bc(\cos\alpha)\beta_{2,3}]$.

located on a crystallographic twofold axis, and the BF_4^- anion was found to be disordered as usual. The presence of one BF_4^- anion per Au_4Ir cluster was confirmed by elemental analysis. The final positional and thermal parameters of the refined atoms appear in Table II and as supplementary material.[21] The labeling scheme for the cation is presented in Figure 1. A table of observed and calculated structure factor amplitudes is included as supplementary material.[21]

Results and Discussion

$[IrAu_3(PPh_3)_5NO_3](BF_4)$ (**2**)[1,14] reacted rapidly with 1 atm of H_2 in CH_2Cl_2 to form the dihydrido metal cluster $[IrAu_4(H)_2(PPh_3)_6](BF_4)$ (**3**) in moderate yield. The structure of **3** was determined in the solid and solution phases by single-crystal X-ray diffraction and by NMR spectroscopy, respectively.

Description of the Solid-State Structure. The crystal of **3** was found to be a CH_2Cl_2 solvate with formulation $[IrAu_4(H)_2(PPh_3)_6]BF_4 \cdot 1.5CH_2Cl_2$. The structure consists of discrete cations, anions, and CH_2Cl_2 solvate molecules. There are no unusually short contacts between these species. Figure 1 shows an ORTEP drawing of the $IrAu_4(PPh_3)_6$ core and includes atom labels and selected distances and angles. An ORTEP drawing of the entire cation and a table of all bonded distances and angles are included as supplementary material.[21]

The structure of the cation consists of an approximately trigonal-bipyramidal (TBP) $IrAu_4$ core with Au3 and Au4 occupying the axial positions. The major deviation from ideal TBP geometry

(21) See paragraph at end of paper regarding supplementary material.

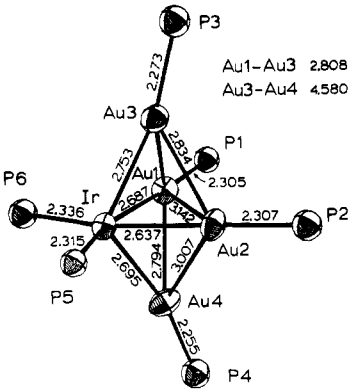

Figure 1. ORTEP drawing of the $IrAu_4P_6$ core in **3** with 50% probability ellipsoids. The esd's in M–M and M–P distances are 2 and 8, respectively, in the last significant figure. Selected angles (deg) where the numbers refer to Au atoms are: 1–Ir–2 = 72.33; 1–Ir–P5 = 163.0; 2–Ir–P6 = 162.4; 3–Ir–4 = 114.44; 1–Ir–3 = 62.14; 2–Ir–3 = 63.40; 1–Ir–4 = 62.53; 2–Ir–4 = 68.64; Ir–1–2 = 53.09; Ir–2–1 = 54.58; Ir–1–P1 = 176.0; Ir–2–P2 = 169.7; 3–1–4 = 109.70; 3–2–4 = 103.26; Ir–3–1 = 57.79; Ir–3–2 = 56.30; 1–3–2 = 67.68; Ir–3–P3 = 165.4; Ir–4–1 = 58.60; Ir–4–2 = 54.76; 1–4–2 = 65.48; Ir–4–P4 = 166.9. Esd's in the last significant figure for M–M–M and M–M–P angles are 5 and 2, respectively. The phenyl ring carbon atoms are labeled C1A, C2A, ..., C6S for phenyl rings A, B, C (attached to P1), D, E, F (P2), ..., Q, R, S (P6).

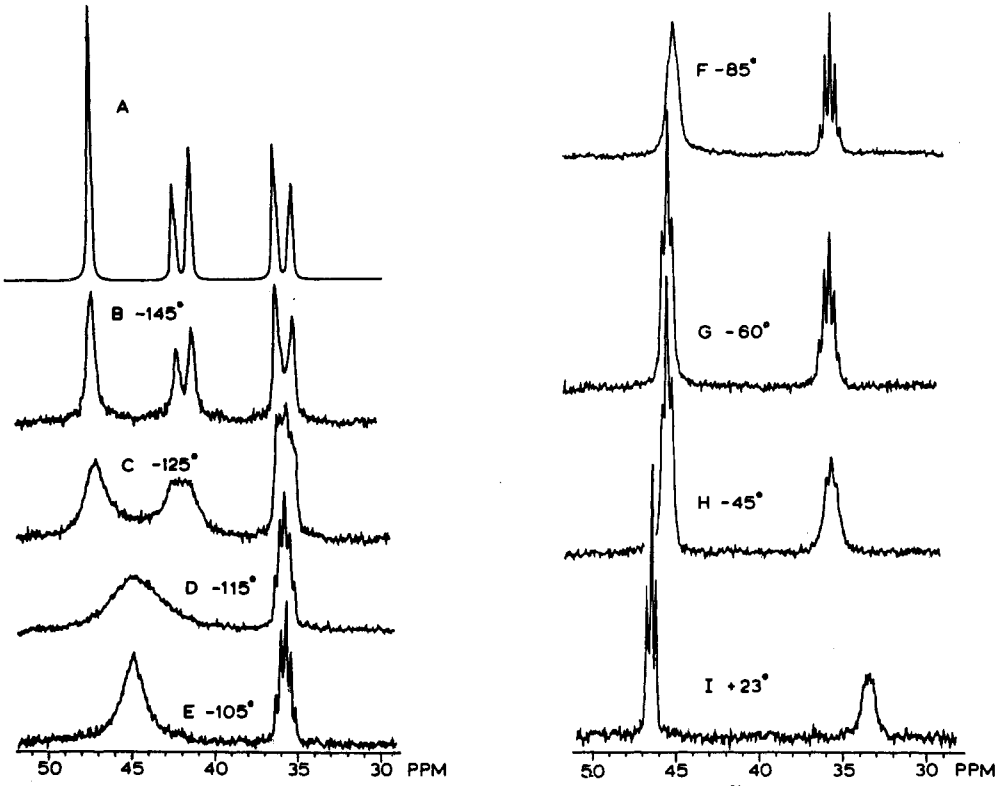

Figure 2. $^{31}P\{^1H\}$ NMR spectra recorded at various temperatures of **3** (spectra B–I) and a simulated ^{31}P NMR spectrum of an $AA'BB'C_2$ spin system (spectrum A). The coupling constants used for the calculated spectrum are $J(P_A–P_B) = J(P_A–P_{B'}) = 118$ Hz, $J(P_A–P_{A'}) = 30$ Hz, $J(P_{A'}–P_{B'}) = J(P_A–P_B) = J(P_C–P_C) = J(P_C–P_{B'}) = 10$ Hz, and $J(P_C–P_C) = J(P_B–P_{B'}) = 0$ Hz. A line broadening of 12 Hz was applied to this spectrum. The spectra B–H were obtained in a 1:1 (v/v) mixture of CH_2Cl_2 and $CHClF_2$. Spectrum I was obtained in CH_2Cl_2 solution.

is caused by the shorter Ir–Au distances (average 2.690 (2) Å) compared with the bonded eq–eq and eq–ax Au–Au separations (average 2.920 (2) Å). Thus, the Au1–Au2 distance (3.142 (2) Å) in the IrAu1Au2 equatorial plane is long and the Au1–Ir–Au2 angle (72.33 (5)°) is opened compared with the Ir–Au1–Au2 and Ir–Au2–Au1 angles (53.09 (4) and 54.58 (4)°, respectively). This results in a TBP that is slightly flattened toward the Ir atom but not enough to approach square-pyramidal (SP) geometry. The dihedral angle between the Au1Au2Au3 and Au1Au2Au4 planes is 33° while a value of 0° is required by SP geometry.

The phosphorus atoms which are bonded to the metals in the equatorial plane lie approximately within this plane. The deviations of P1, P2, P5, and P6 from the IrAu1Au2 plane are 0.05 (1), 0.11 (1), –0.02 (1), and 0.10 (1) Å, respectively. The Ir–Au distances (average 2.690 (2) Å) are comparable to distances observed in other known Ir–Au phosphine clusters (2.685 (1) Å in **1**[1] and 2.641 (1) Å in **2**[13]). The bonded Au–Au separations (average 2.920 (2) Å including Au1–Au2 and average 2.860 (2) Å excluding Au1–Au2) are long compared to distances in other Ir–Au phosphine clusters (2.728 (1) Å in **1**[1] and 2.767 (1) Å in **2**[13]). The long Au–Au distances in **3** probably result from the higher coordination number for Au in **3** (coordination number 4, excluding possible Au–hydride interaction) compared with a coordination number of 3 in **1** and **2**.

The Au–P vectors are approximately trans to the Ir–Au vectors (average Ir–AuX–PX angle 169.5 (2)°). This has also been observed in **1** and **2** and shows that Ir–Au bonding is more important than Au–Au bonding in such clusters. The geometry about the Au atoms is therefore not tetrahedral (average Au–AuX–PX angle 128.2 (2)°). The average Au–P and Ir–P distances are 2.290 (8) and 2.330 (8) Å, respectively, and are similar to values observed in **1** (2.272 (4) and 2.343 (4) Å, respectively)[1] and **2** (2.266 (4) and 2.329 (4) Å, respectively).[13]

The positions of the two hydride ligands could not be determined in the X-ray analysis. The most reasonable positions for these hydrides based on the solid-state structure is bridging the Ir–Au3 and Ir–Au4 bonds or terminally bonded to the Ir atom approximately trans to Au3 and Au4. The bridging description is most consistent with NMR data obtained in solution (vide infra). Therefore, the coordination number for the Ir is 8. The Au1–Ir–P5 and Au2–Ir–P6 angles are 163.0 (2) and 162.4 (2)°, respectively, while the Au1–Ir–Au2 and P5–Ir–P6 angles are 72.33 (5) and 106.8 (3)°, respectively.

Description of the Solution Structure and NMR Properties. Complex **3** has been characterized in solution by $^{31}P\{^1H\}$ and ^1H NMR spectroscopy. These data were consistent with the overall formulation of **3** and with its solid-state structure; however, variable-temperature $^{31}P\{^1H\}$ NMR experiments indicated that **3** underwent a rapid fluxional process in solution.

The solid-state structure of the metal phosphine core of **3** is shown in Figure 1 and consists of an approximate TBP geometry (vide supra) that has approximate C_{2v} symmetry. The room-temperature $^{31}P\{^1H\}$ NMR spectrum of **3** with CH_2Cl_2 as solvent was not entirely consistent with this structure and showed only two resonances (see trace I in Figure 2). The triplet resonance is assigned to the gold phosphines (46.5 ppm, int = 2) and the broad unresolved resonance to the iridium phosphines (33.6 ppm, int = 1). Variable-temperature $^{31}P\{^1H\}$ NMR experiments with $CH_2Cl_2/CHClF_2$ as solvent showed that **3** underwent a rapid rearrangement in solution in which the axial and equatorial gold phosphine sites were interconverted. These $^{31}P\{^1H\}$ NMR spectra are shown in Figure 2. As the temperature was lowered to ca. –60 °C, the broad iridium phosphine resonance sharpened into a well-resolved quintet and the gold phosphine triplet remained sharp. At lower temperatures the gold phosphine resonance broadened and split into two resonances while the iridium phosphine quintet broadened and changed into an apparent doublet. The slow-exchange limiting spectrum was reached at –145 °C and is shown in trace B of Figure 2. This spectrum consisted of a singlet due to P3 and P4 (47.3 ppm, int = 1), an apparent doublet due to P1 and P2 (41.8 ppm, $J(P–P) = 118$ Hz, int = 1), and another apparent doublet due to P5 and P6 (35.8 ppm, $J(P–P) = 118$ Hz, int = 1). ^{31}P NMR simulation studies have shown that this pattern is consistent with an $AA'BB'C_2$ spin system in which $J(A'–B)$ and $J(A–B')$ are equal to 118 Hz and are much greater in magnitude than the remaining spin–spin

coupling constants, which are not resolved. The C phosphines are the axial P3 and P4, and the A and B phosphines are the equatorial P1, P2 and P5, P6, respectively. An example of one of these simulated spectra is shown in trace A of Figure 2.[22] $J(A'-B)$ is equal to the separation of the two resonances making up each doublet.

The magnitude of $J(A'-B)$ is consistent with the approximately linear P_A–Au–Ir–P_B stereochemistry for P1, P5 and P2, P6 found in the solid-state structure of **3** (vide supra) and supports the assignment of a similar structure in solution. Although very few three-bond trans P–P coupling constants for linear P–M–M–P geometries have been reported, van der Velden[23] observed a value of 194 Hz for a linear P–Au–Au–P arrangement in $[Au_8(PPh_3)_8]^{2+}$ and Balch has reported values in the range of 160–180 Hz for a series of dimeric Pt complexes of the type[24]

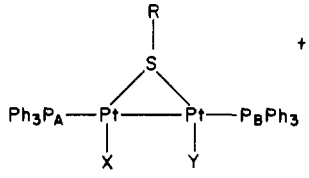

The magnitudes of these coupling constants are somewhat larger than that observed for **3**. This could be a result of the deviation of the P–Au–Ir–P geometry from linearity in **3** (average $Au_{1,2}$–Ir–$P_{5,6}$ angle is 162.7 (2)° and average Ir–$Au_{1,2}$–$P_{1,2}$ angle is 172.9 (2)°). P–P coupling constants are very sensitive to these angles. For example, the P–P coupling constants in other Au–Ir clusters where the Au–Ir–P angle is ca. 90° are in the range of 0–10 Hz.[1,13] The remaining spin–spin coupling constants in **3** could not be determined unambiguously; however, the use of the accepted values 0–10 Hz for the nonlinear P–Ir–Au–P arrangements,[1,13] 15–40 Hz for the cis IrP_2 arrangement,[25] and 0–14 Hz for the P–Au–Au–P arrangements[1,13,23,26] gave good results in the calculated spectra.

When this solution was warmed to −60 °C, the two gold phosphine resonances broadened, coalesced, and then sharpened into a triplet (45.4 ppm, J = 36 Hz) while the iridium phosphine resonance broadened and sharpened into a quintet (35.7 ppm, J = 36 Hz) as shown in traces E–G. This behavior is entirely consistent with the rapid interconversion of axial and equatorial gold phosphine sites and the averaging of the P_{Au}–P_{Ir} coupling constants. The gold phosphine resonance appears as a triplet due to coupling with the two equivalent iridium phosphines, and the iridium phosphine resonance appears as a quintet due to coupling with the four averaged gold phosphines.

Continued warming of this solution above −45 °C showed the expected sharpening of the triplet; however, the Ir phosphine resonance broadened slightly as shown in spectra H and I. This broadening was reversible as the temperature was repeatedly lowered and raised. The $^{31}P\{^1H\}$ NMR spectrum of **3** recorded with use of acetone as solvent was qualitatively similar and did not show any further broadening or sharpening of this resonance up to 65 °C, and the triplet due to the gold phosphines remained sharp. The reason for this broadening of the iridium phosphine resonance is not understood but cannot be due to an intermolecular exchange process since P_{Ir}–P_{Au} coupling is maintained.

The rapid interconversion of gold phosphine sites in gold phosphine clusters in solution at room temperature is now well established. These exchange processes are very facile and are believed to occur through small conformational changes in the gold skeleton rather than through a migration of phosphines over a rigid gold skeleton.[2,23] A reasonable mechanism for the rearrangement process in **3** involves the movement of the axial Au–P's toward the equatorial plane and the movement of the equatorial Au–P's away from each other along the equatorial Au–Au vector. The transition-state geometry would be square pyramidal with the iridium atom occupying the apical position. The Ir–P's must also rotate 90° about the C_2 axis during the rearrangement in order to achieve the original configuration. This mechanism is likely to be a very facile process since it involves the breaking of only one formal Au–Au (equatorial) bond. X-ray structure results show that this equatorial Au–Au interaction is long and is therefore weakened in the ground state (vide supra).

Although the hydride ligands were not located in the X-ray structure of **3**, their presence was confirmed by the observation of a multiplet at −5.71 ppm in the room-temperature ^1H NMR spectrum recorded with use of acetone-d_6 as solvent. The formulation of **3** as a dihydride was based upon integration data that related the areas of the ^{31}P resonances of **3** to the ^{31}P resonance of internal standard trimethyl phosphate (TMP) and the area of the TMP ^1H resonance to the area of the hydride resonance of **3**. This experiment gave 1.9 ± 0.1 hydrides per cluster. The dihydride formulation is also consistent with the 1+ charge (one BF_4^- counterion per cluster) and the requirement that **3** is diamagnetic.

Unfortunately, an unambiguous assignment of the hydride positions in **3** cannot be made. Since very few examples of stable complexes that contain Au–H interactions are known, the determination of a terminal or bridging bonding mode is of interest. Ir–H stretches that are characteristic of terminal hydrides were absent in the KBr infrared spectrum of **3**. The ^1H chemical shift of the hydride multiplet (−5.71 ppm) was also characteristic of a bridging hydride;[6,7,13,27] however, these criteria must be used with caution in assigning the bonding mode of a hydride.[13] Selective $^1H\{^{31}P\}$ decoupling experiments conducted at ambient temperature with use of acetone-d_6 as solvent showed that the multiplet at −5.71 ppm consisted of a single hydride resonance. Decoupling of the Ir phosphorus atoms gave a quintet with $J(P_{Au}–H)$ = 13.5 Hz, and decoupling of the Au phosphorus atoms gave a broad triplet with $J(P_{Ir}–H) \approx 9$ Hz. The magnitude of $J(P_{Au}–H)$ is similar to that reported for the terminal Ir hydrides in other Ir/Au clusters,[6,13] and a Au–H–Ir bridging interaction is expected to give rise to a larger $J(P_{Au}–H)$ value. However, this coupling constant is an average of all four P_{Au}–H coupling constants due to the rapid rearrangement of **3** in solution. Thus, it is possible that the two hydrides occupy bridging positions and that $J(P_{Au}–H)$ for the bridging interaction is much larger than 13.5 Hz. Low-temperature (−90 °C) ^1H NMR studies of **3** showed only a slight broadening in the hydride multiplet, and this result is also consistent with the rapid rearrangement of **3**, which is fast even at −90 °C. The results of the low-temperature $^{31}P\{^1H\}$ NMR experiment conducted at −145 °C suggest that the two hydrides occupy positions that preserve the C_2 symmetry, but this conclusion is valid only if the hydrides are not rapidly scrambling at this temperature. Thus, the hydride positions remain uncertain but are most likely bridging the Ir–Au3 and Ir–Au4 bonds.

The reaction of **2** with H_2 is not well understood. Gold phosphine monomers and gold phosphine clusters have not been reported to undergo similar cluster growth reactions under H_2, so it is very likely that H_2 activation takes place at the Ir atom. The ability of Ir complexes to oxidatively add H_2 is well-known, whereas there are very few examples of stable complexes that contain Au–H interactions. An understanding of the mechanism of this unusual reaction is obviously important, and work is in progress toward this end.

Acknowledgment is made to the National Science Foundation (NSF Grant CHE-81-08490) and to NATO for a travel grant. The Johnson-Matthey Co. is acknowledged for a generous loan of $IrCl_3$. We thank Professor J. J. Steggerda and his research

(22) The high-resolution calculated spectra were more complicated than shown in this spectrum and contained much more fine structure; however, the use of experimentally determined line widths obscured these small splittings.
(23) van der Velden, J. W. A. Ph.D. Thesis, University of Nijmegen, Nijmegen, The Netherlands, 1983.
(24) Hunt, C. T.; Matson, G. B.; Balch, A. L. *Inorg. Chem.* **1981**, *20*, 2270.
(25) Sanger, A. R. *J. Chem. Soc., Dalton Trans.* **1977**, 120.
(26) Vollenbroek, F. A.; van den Berg, J. P.; van der Velden, J. W. A.; Bour, J. J. *Inorg. Chem.* **1980**, *19*, 2685.
(27) Wang, H. H.; Pignolet, L. H. *Inorg. Chem.* **1980**, *19*, 1470.

group in Nijmegen, The Netherlands, for many helpful suggestions and discussions. A.L.C. is the recipient of an NSF Graduate Fellowship.

Registry No. 2, 93895-69-3; 3, 96705-42-9; Au, 7440-57-5; Ir, 7439-88-5.

Supplementary Material Available: Figures of the molecular structure of 3 with a complete labeling scheme and an ORTEP stereoview of the cluster core and tables of distances and angles, general anisotropic temperature factor expressions, weighted least-squares planes, torsional angles, and observed and calculated structure factor amplitudes for 3 (26 pages). Ordering information is given on any current masthead page.

Contribution from the Research School of Chemistry, The Australian National University, Canberra, ACT 2601, Australia, and Division of Inorganic Chemistry, Kemisk Institut, Aarhus Universitet, DK-8000 Aarhus C, Denmark

Synthesis and Properties of Novel Cobalt(III) and Nickel(II) Complexes with Coordinated Azetidine Nitrogens: Crystal Structure of *mer*-Tris(3-(aminomethyl)-3-methylazetidine)cobalt(III) Chloride Trihydrate

RODNEY J. GEUE,[1a] MARK G. McCARTHY,[1a] ALAN M. SARGESON,*[1a] PALLE JØRGENSEN,[1b] RITA G. HAZELL,[1b] and FINN KREBS LARSEN[1b]

Received June 13, 1984

Syntheses of the new amine 3-(aminomethyl)-3-methylazetidine (ama) and the complexes *mer*-$[Co(ama)_3]^{3+}$ and $[Ni(ama)_3]^{2+}$ are described, and the crystal structure of the *mer*-$[Co(ama)_3]Cl_3 \cdot 3H_2O$ isomer is reported. This structure is triclinic, space group $P\bar{1}$, with $a = 13.926$ (5) Å, $b = 10.303$ (5) Å, $c = 9.804$ (4) Å, $\alpha = 116.51$ (3)°, $\beta = 91.41$ (2)°, $\gamma = 105.15$ (2)°, and $Z = 2$. The final $R(F) = 0.043$ for 2303 reflections with $(\sin\theta)/\lambda \leq 0.60$ Å^{-1}. The nitrogen atom configuration around Co is close to a regular octahedron with Co–N distances in the range 1.973 (5)–2.024 (5) Å. The ligand field absorption spectrum of the $[Co(ama)_3]^{3+}$ ion is shifted to exceptionally low energies, $\lambda_{max} = 513$ nm (crimson), compared with those of other tris(diamine)cobalt(III) complexes, $\lambda_{max} \approx 465$–475 nm (yellow-orange), presumably because of the longer Co–N bonds and orbital constraints at the azetidine donor atoms. The cobalt complex is stable in ~5 M DCl over several days but is susceptible to base hydrolysis (pH >3). The coordinated azetidine ring of the chelate does not rupture under the hydrolysis conditions and is apparently stable to nucleophilic attack by OMe^- and CN^- prior to ligand substitution reactions.

Introduction

Cobalt(III) tris(diamine) complexes containing five-, six-, and seven-membered chelate rings have shown some variations in Co(III)–N bond lengths and significant distortions from octahedral symmetry.[2] Average cobalt–nitrogen distances for accurately determined crystal structures range from 1.964 (1) Å in (+)-$[Co(en)_3]Cl((+)\text{-}C_4H_4O_6)\cdot 5H_2O$[3] (en = ethylenediamine) to 1.991 (5) Å in $(+)_{589}$-$[Co(tmd)_3]Br_3$[4] (tmd = 1,4-butanediamine) and N–Co–N bond angles from 91.0° in $(-)_{589}$-$[Co(tn)_3]Cl_3 \cdot H_2O$[5] (tn = 1,3-propanediamine) to 84.2° in $(+)_{589}$-$[Co((-)\text{-chxn})_3]Cl_3 \cdot H_2O$ (chxn = *trans*-1,2-cyclohexanediamine).[6] Both the chelate ring size and flexibility appear to be important in determining the structural characteristics of the CoN_6 chromophore in a given complex. We supplement these results with a study of the synthesis, structure, and properties of a novel cobalt(III) tris(diamine) complex and the synthesis of its nickel(II) analogue in which the ligand (ama) contains a strained azetidine ring. Coordination of the azetidine ring nitrogen to the relatively inert Co(III) center might be expected to activate the adjacent strained ring carbons to nucleophilic attack. The ligand forms an unusually rigid six-membered chelate ring, which could be suitable for probing the reactivity and stereochemistry of nucleophilic addition to such carbon centers.

Experimental Section

All chemicals used were of analytical grade. ^{1}H NMR spectra were recorded with a JEOL JNM-FX-200 Fourier transform spectrometer or a JEOL JNM-PMX-60 spectrometer for the hydrolysis experiments at 25 °C with sodium 3-(trimethylsilyl)propanesulfonate (NaTPS) as internal standard. ^{13}C NMR spectra were recorded with a JEOL JNM-FX-200 Fourier transform spectrometer (INEPTR spectrum[7]) at 27 °C or a JEOL JNM-FX-60 Fourier transform spectrometer at 25 °C relative to 1,4-dioxane as internal standard (s denotes a singlet, br a broad, and m a multiplet resonance). Chemical shifts are reported as positive downfield from the standard. A Cary 118 spectrophotometer (UV/vis) and a Cary 17 spectrophotometer (near-IR) were used to measure absorption spectra.

A 6-L high-pressure autoclave suitable for reaction temperatures and pressures to 350 °C and 350 atm was employed for the ligand synthesis. Bio-Rad analytical Dowex 50W-X2 (200–400 mesh, H^+ form) and SP-Sephadex (C-25, Na^+ form) ion-exchange resins were used for the cation-exchange chromatography.

All evaporations were carried out under reduced pressure (≤20 torr) with Büchi rotary evaporators such that the temperature of the solution did not exceed 25 °C.

pK_a values were determined by pH titration[8] of ama·2HCl with 0.1 M KOH under nitrogen at 20 °C.

Syntheses. 3-(Aminomethyl)-3-methylazetidine (ama). Ethylidynetris(methylene benzenesulfonate) (500 g) was prepared as described previously[9] and slowly heated with liquid NH_3 (4 L) in a steel autoclave fitted with an enameled sleeve (6-L volume). After 12 h with intermittent stirring the temperature reached 100 °C and the pressure ~60 atm. These conditions were maintained for 12 h before the system was allowed to cool to ~20 °C. The temperature of the reaction mixture was monitored and regulated with a thermocouple probe attached to a temperature control unit incorporated in the heating circuit. *Caution!* It is mandatory to ensure that no significant area of the autoclave interior exceeds a temperature of 132.4 °C at any time (the critical temperature of NH_3) and rapid nonequilibrium heating is not advisable. The NH_3 was removed through a valve connected to an efficient water aspirator, and the autoclave was warmed to 30–40 °C during this period. The pale yellow syrupy residue was dissolved in H_2O (10 L), and HCl (~4 M)

(1) (a) The Australian National University. (b) Aarhus Universitet.
(2) Saito, Y. *Top. Stereochem.* **1978**, *10*, 95.
(3) Templeton, D. H.; Zalkin, A.; Ruben, H. W.; Templeton, L. K. *Acta Crystallogr., Sect. B: Struct. Crystallogr. Cryst. Chem.* **1979**, *B35*, 1608. Magill, L. S.; Korp, J. D.; Bernal, I. *Inorg. Chem.* **1981**, *20*, 1187.
(4) Sato, S.; Saito, Y. *Acta Crystallogr., Sect. B: Struct. Crystallogr. Cryst. Chem.* **1975**, *B31*, 1378.
(5) Nagao, R.; Marumo, F.; Saito, Y. *Acta Crystallogr., Sect. B: Struct. Crystallogr. Cryst. Chem.* **1973**, *B29*, 2438.
(6) Kobayashi, A.; Marumo, F.; Saito, Y. *Acta Crystallogr., Sect. B: Struct. Crystallogr. Cryst. Chem.* **1972**, *B28*, 2709.
(7) "JEOL Application Note"; JEOL Analytical Instruments Inc.: Akishima, Japan, Jan 1981; No. 2.
(8) Albert, A.; Serjeant, E. P. "The Determination of Ionization Constants"; Chapman and Hall: London, 1971.
(9) (a) Fleisher, E. B.; Gebala, A. E.; Levey, A.; Tasker, P. A. *J. Org. Chem.* **1971**, *36*, 3042. (b) Geue, R. J.; Searle, G. H. *Aust. J. Chem.* **1983**, *36*, 927.

0020-1669/85/1324-2559$01.50/0